A LEAST SQUARES APPROXIMATION OF ANNULAR FLOW

R. Loendersloot and R. Akkerman

Composites Group, University of Twente,
P.O. Box 217, 7500 AE Enschede, The Netherlands: r.loendersloot@ctw.utwente.nl

SUMMARY: A first step in the prediction of the permeability of RTM preforms is to solve the Stokes flow problem in domains with an arbitrary cross-section. This can be used to model annular flow parallel to a fibre or a tow as well as the transverse flow. Here the parallel flow problem is solved using a least squares approximation for the boundary conditions while minimising the dissipative work of the fluid.
The convergence of the method is tested for various penalty factors for the boundary interpolation and for various number of collocation points for the boundary condition. Convergence is obtained easily.
The algorithm is applied on a circular and a square flow domain. The flow rate in a circular domain can be determined in a closed form as well and is therefore used as a test case. The results of the square domain are compared with the results of a FE-analysis.
The effect of the eccentricity of the fibre is analysed. The results of the circular and square domain show similar behaviour. The observed behaviour corresponds with the behaviour found in the literature.
The method presented is fast and accurate. It is a useful method to analyse flow along and perpendicular to fibres. To compute the transverse flow only minor adaptations are required.

KEYWORDS: minimised dissipative work, resin flow, parallel flow, permeability, eccentricity

INTRODUCTION

Resin Transfer Moulding (RTM) is being applied increasingly as the manufacturing process of high performance composites. Consequently, significant research effort has been devoted to mould filling and fibre impregnation during this type of Liquid Composite Moulding process. The main objective of the investigations is to improve the process-readiness of RTM.
Accurate flow simulations are a useful tool in finding the optimal process parameters, for example the flow rate and inlet pressure, and optimal gate and vent locations. Incorrect process parameters or badly chosen gate and vent locations may cause the formation of dry spots and voids in the preform, which has unacceptable consequences for the material properties of the composite in terms of its strength and fatigue resistance.
According to Darcy, the flow through a porous medium is governed by the pressure drop over the medium, the viscosity of the fluid and the permeability of the medium. Experimental and

numerical methods to determine the permeability of a preform have been developed $[1-11]$. However, in general, the experimental data suffers from instability and low repeatability and low reproducibility $[1]$: despite the vast amount of experimental data, it is not possible yet to produce reliable permeability data of a given preform. Nevertheless, experimental studies of the factors affecting the permeability of a preform have revealed that the architecture of the preform influences the permeability significantly $[2-6]$. These investigations consider the effects on the permeability of the type of reinforcement architecture (unidirectional, woven fabrics or other textiles) and the curvature of the moulds. All results confirm that the permeability is not only a function of the overall fibre content, but certainly also of the macroscopic and microscopic distribution of the fibres in the domain.

Although there are some examples of studies of the permeability in three dimensions, $[7,8]$, most experiments concern flat preforms, from which only the in-plane permeability can be extracted. When analysing the resin flow in thicker preforms, these experiments do not provide sufficient information.

Apart from the experiments, several numerical models of the resin flow have been proposed $[8-11]$. Although the models differ significantly on some aspects, all agree on the fact a fibre texture has to be considered as a double porous medium: resin flow occurs around the fibre bundles (meso scale) and inside the fibre bundles (micro scale). Poiseuille flow and capillary flow respectively determine the flow characteristics. However, with increasing fibre content, the influence of the capillary flow has to be accounted for on the meso scale as well.

The permeability is assumed to be known locally in the proposed numerical models. Different methods are used to compute the overall permeability from the local permeabilities. The resin flow as well as the fibre architecture on local levels is far less complicated than the overall resin flow and fibre architecture. Therefore, relatively simple equations can be used to determine the local permeability. The resin flow parallel or perpendicular to fibre bundles is governed by the Stokes equation. The flow parallel and across arrays of cylinders has been investigated extensively. The effect of the fibre arrangement has played an important role in these projects $[4,12-15]$. Lubrication theory and capillary theory have been used to solve the Stokes equation.

Here, a method to compute the flow parallel to the fibre bundles is presented. A circular and a rectangular domain are defined, containing a circular solid core, representing an impermeable fibre bundle. In this geometry the effect of the fibre content on the permeability can be studied by varying the relative size of the core. The effect of the fibre distribution is examined by varying the position of the core within the external boundary.

In the first part the theory used is presented briefly. The Stokes equation is solved using the general solution of a Laplacian differential equation. The coefficients of the general solution are determined using a least squares approximation for the boundary conditions and the concept of minimum dissipated work. In the following section the theory is applied on the circular and square domain. The flow profile in the circular domain can be determined in closed form and thus serves as a good test case for the approximation method. The paper is finished with the conclusions.

THEORETICAL BACKGROUND

General Fluid Mechanics

The fluid mechanics used are presented briefly below. The theory can be found in a more elaborate form in many textbooks, among which $[12,16]$. In general a fluid problem is solved by using:

- the conservation of mass;
- the impulse balance (Newton's second law);
- the conservation of energy;
- constitutive equations;
- boundary conditions.

The conservation of mass, also known as continuity equation, is given by:

$$\frac{\mathrm{D}\rho}{\mathrm{D}t} = \rho(\nabla \cdot \underline{u}), \tag{1}$$

with ρ the density of the fluid, t the time and $\underline{u}$ the velocity of the fluid. $\mathrm{D}/\mathrm{D}t$ denotes the material derivative.
The conservation of momentum reads:

$$\rho\frac{\mathrm{D}\underline{u}}{\mathrm{D}t} = \nabla \cdot \underline{\underline{\sigma}} + \rho\underline{g}, \tag{2}$$

with $\underline{g}$ the specific gravity and $\underline{\underline{\sigma}}$ the stress tensor:

$$\underline{\underline{\sigma}} = -p_h\underline{\underline{I}} + \underline{\underline{\sigma}}_d, \tag{3}$$

with p_h the hydrostatic pressure and $\underline{\underline{\sigma}}_d$ the deviatoric stress tensor.
The change of energy within the system can only be caused by a heat source or by the motion of the fluid:

$$\rho\frac{\mathrm{D}U}{\mathrm{D}t} = -\nabla \cdot \underline{q} + \underline{\underline{\sigma}} : \nabla\underline{u}, \tag{4}$$

with U the specific internal energy and $\underline{q}$ the heat flow. The last term in Eqn. 4 represents the mechanical work. On thermodynamical considerations, an allowable velocity profile $\underline{u}$, satisfying the conservation laws of mass and momentum (Eqn. 1 and Eqn. 2), will satisfy the condition of minimised dissipative work within the system.
The resin is assumed to behave Newtonian and to be incompressible. Since the flow rate is low, the flow is assumed to be steady, uniform and laminar. Isothermal flow is observed.
The constitutive equation relates the rate of deformation to the stress. For incompressible Newtonian fluids, this is given by:

$$\underline{\underline{\sigma}}_d = 2\mu\underline{\underline{D}}, \tag{5}$$

with μ the viscosity of the fluid and $\underline{\underline{D}}$ the rate of deformation, defined as the symmetric part of the velocity gradient $\underline{\underline{L}}$:

$$\underline{\underline{L}} = \underline{u}\,\underline{\nabla} = \frac{1}{2}\left((\underline{u}\,\underline{\nabla}) + (\underline{u}\,\underline{\nabla})^T\right) + \frac{1}{2}\left((\underline{u}\,\underline{\nabla}) - (\underline{u}\,\underline{\nabla})^T\right) = \underline{\underline{D}} + \underline{\underline{W}}. \tag{6}$$

The anti-symmetric part is defined as $\underline{\underline{W}}$, the vorticity.
The integration constants resulting from solving the differential equations above, depend on the boundary conditions. Either Dirichlet or Neumann boundary conditions (or a combination) can be assumed. Furthermore, the velocity is assumed to be independent of the axial coordinate, whereas the pressure is assumed to be a function of the axial coordinate only. Gravitation is not accounted for.

General Solution For Axial Flow

The general equations are reduced to a two dimensional problem, by applying the above assumptions. The velocity field is expressed in terms of the axial velocity component only. Using the momentum equation, Eqn. 2, and the constitutive equation, Eqn. 5, it can be derived that the axial velocity field has to satisfy:

$$u(r,\theta) = \frac{1}{4\mu}\frac{\mathrm{d}p}{\mathrm{d}x}r^2 + \psi, \tag{7}$$

with ψ an arbitrary function obeying the boundary conditions and:

$$\nabla^2\psi = 0. \tag{8}$$

Note that the cylinder coordinates (x,r,θ) have been used to derive Eqn. 7. The problem is now reduced to finding a function ψ, i.e. solving a homogeneous second order partial differential equation. The general solution for ψ is [17]:

$$\begin{aligned}\psi &= a_0 + b_0\ln r + \sum_{k=1}^{\infty}\left(a_k r^k\cos k\theta + b_k r^k\sin k\theta + c_k r^{-k}\cos k\theta + d_k r^{-k}\sin k\theta\right)\\ &= \{F\}\cdot\{\alpha\},\end{aligned} \tag{9}$$

with $\{F\}$ the set of basic functions and $\{\alpha\}$ the vector of constants a_k, b_k, c_k and d_k. These constants are determined using the principle of minimum work. The total mechanical work is found by integrating the last term of Eqn. 4 over the cross-sectional area of the flow domain:

$$\begin{aligned}W_{disp} &= \int_A w_{disp}\mathrm{d}A = \iint_A \underline{\underline{\sigma}} : \underline{\nabla}\,\underline{u}\, r\mathrm{d}r\mathrm{d}\theta = \iint_A 2\mu\underline{\underline{D}} : \underline{\underline{D}}\, r\mathrm{d}r\mathrm{d}\theta\\ &= \mu\iint_A\left(\left(\frac{\partial u(r,\theta)}{\partial r}\right)^2 + \left(\frac{1}{r}\frac{\partial u(r,\theta)}{\partial\theta}\right)^2\right) r\mathrm{d}r\mathrm{d}\theta.\end{aligned} \tag{10}$$

The axial velocity field, as defined in Eqn. 7, is found by minimisation of this dissipative work. Two extra terms are added to satisfy the boundary conditions. A weak formulation is used in which the boundary conditions only have to be obeyed in a limited number of interpolation points instead of on the complete boundary. The modified potential Φ is defined as:

$$\Phi = W_{disp} + P_1\sum_{i=1}^{m_D}\left(\{F_\Gamma\}_i\cdot\{\alpha\} + \frac{1}{4\mu}\frac{\mathrm{d}p}{\mathrm{d}x}r_{\Gamma_i}^2 - u_\Gamma\right)^2 + P_2\sum_{i=1}^{m_N}\left(\left\{\frac{\partial F_\Gamma}{\partial n}\right\}_i\cdot\{\alpha\} - \gamma_\Gamma\right)^2, \tag{11}$$

with m_D and m_N the number of Dirichlet and Neumann interpolation points, P_1 and P_2 weight factors, F_Γ the basic functions at the boundary and u_Γ the prescribed velocities and γ_Γ the prescribed velocity gradient normal to the boundary.
The coefficient vector $\{\alpha\}$ which minimises the dissipated work, is found by solving:

$$\frac{\partial\Phi}{\partial\{\alpha\}} = 0. \tag{12}$$

Expanding Eqn. 12 yields the linear system:

$$[M + M_\Gamma]\cdot\{\alpha\} = \{R + R_\Gamma\}, \tag{13}$$

with:

$$[M] = \iint_A \mu\, r \left(\left\{ \frac{\partial F}{\partial r} \right\}^T \left\{ \frac{\partial F}{\partial r} \right\} + \left\{ \frac{1}{r} \frac{\partial F}{\partial \theta} \right\}^T \left\{ \frac{1}{r} \frac{\partial F}{\partial \theta} \right\} \right) \mathrm{d}r\mathrm{d}\theta; \tag{14}$$

$$[M_\Gamma] = P_1 \sum_{i=1}^{m_D} \left(\{F_\Gamma\}_i^T \{F_\Gamma\}_i \right) + P_2 \sum_{i=1}^{m_N} \left(\left\{ \frac{\partial F_\Gamma}{\partial n} \right\}_i^T \left\{ \frac{\partial F_\Gamma}{\partial n} \right\}_i \right); \tag{15}$$

$$\{R\} = -\iint_A \frac{r^2}{2} \left\{ \frac{\partial F}{\partial r} \right\}^T \mathrm{d}r\mathrm{d}\theta; \tag{16}$$

$$\{R_\Gamma\} = P_1 \sum_{i=1}^{m_D} \left(\left(u_\Gamma - \frac{1}{4\mu} \frac{\mathrm{d}p}{\mathrm{d}x} r_{\Gamma_i} \right) \{F_\Gamma\}_i^T \right). \tag{17}$$

The volumetric flow rate Q follows from integrating the velocity field over the cross-sectional area. Subsequently applying Darcy's law leads to an expression for the permeability K:

$$K = \mu Q \left(\frac{\mathrm{d}p}{\mathrm{d}x} \right)^{-1} = \mu \left(\frac{\mathrm{d}p}{\mathrm{d}x} \right)^{-1} \iint_A \{u(r,\theta)\} \mathrm{d}A; \tag{18}$$

EXAMPLES

The algorithm presented in the preceding section is applied on a circular and a square flow domain. The mathematical packages MAPLE and MATLAB have been used to implement the algorithm and analyse the results. In Fig. 1 both flow domains are shown. The effects of the relative size of the core (the fibre content) and the eccentricity (the fibre distribution) were analysed (see also [12]) in both domains.

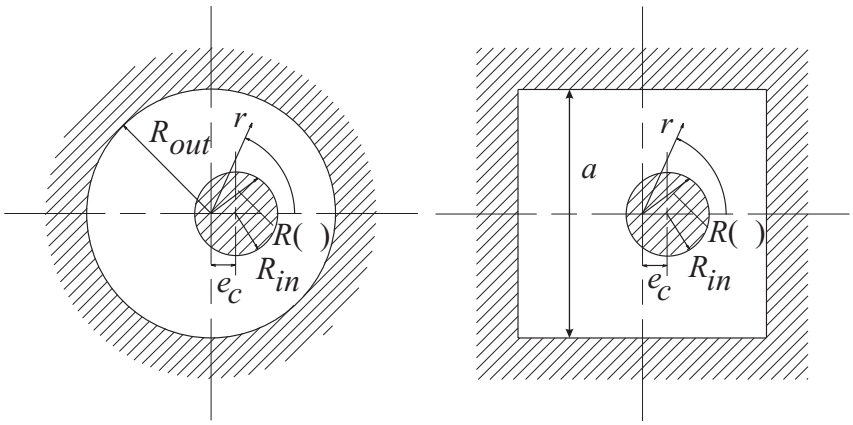

(a) Circular domain (b) Square domain

Fig. 1: The cross-section of both flow domains.

Circular Domain

For the circular domain it is possible to solve the Stokes flow problem directly from the conservation of momentum, Eqn. 2. With no-slip boundary conditions (Dirichlet boundary

conditions) on the inner and outer boundary (R_{in} and R_{out} respectively), the axial velocity is found to be

$$u(r,\theta) = \frac{1}{4\mu}\frac{\mathrm{d}p}{\mathrm{d}x}\left(r^2 - R_{out}^2 + \frac{R_{out}^2 - R_{in}^2}{\ln\dfrac{R_{in}}{R_{out}}} \ln\frac{r}{R_{out}} \right). \tag{19}$$

The least squares approximation has been tested for various penalty factors P_1, for a various number of collocation points for the boundary conditions and various order k of the basic functions. The results are depicted in Fig. 2. The normalised permeability K_n is defined here as the quotient of the permeability according to the least squares approximation and the analytically calculated permeability. The fibre volume fraction is taken equal to 50%.

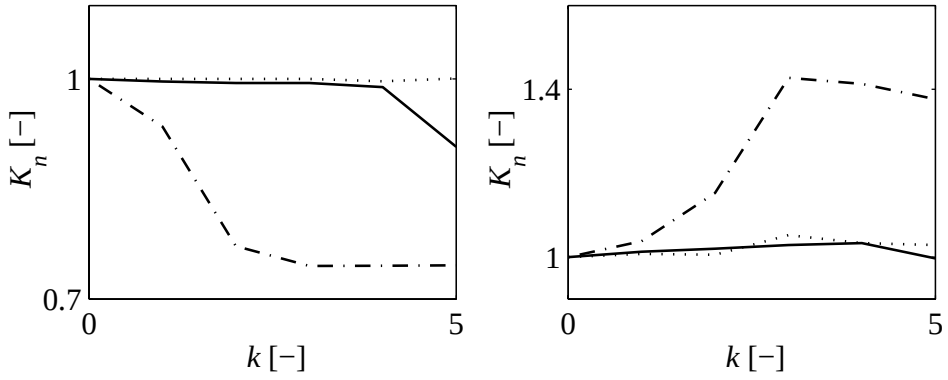

(a) Penalties: - $P_1 = 1$, $\cdots$ $P_1 \ll 1$, -$\cdot$ $P_1 \gg 1$

(b) Number of collocation points on inner and outer boundary: - 2/100, $\cdots$ 100/2, -$\cdot$ 2/2

Fig. 2: The normalised permeability as a function of the order k of the basic functions.

Fig. 2(a) shows the normalised permeability using three different penalty factors P_1 and a constant number of collocation points of 10 on each boundary. The solid line corresponds with P_1 = 1 kg·s·m^{-2}. The dotted line corresponds with P_1 much larger than unity, i.e. the effect of the minimisation of dissipated work is negligible. The least squares solution starts to deviate from the analytical solution only for a relative high order of the basic functions. Increasing the number of collocation points will be sufficient to improve the solution. When the effect of the minimisation of work is increased, i.e. choosing P_1 very small (dash-dotted line), the solution converges to approximately 0.75. The smoothing effect causes the velocity to be reduced to zero on the symmetry boundaries (the circular domain is analysed between $\theta \in [0, \pi/4]$). Applying Neumann boundary points on the symmetry boundaries improves the solution.

In Fig. 2(b) the number of collocation points is varied, with P_1 taken equal to unity. The solid line shows the normalised permeability calculated with 2 collocation points on the inner and 100 on the outer boundary. For the dotted line, 100 points are used on the inner boundary and 2 on the outer. The dash-dot line is calculated using 2 collocation points on each boundary. In this case, the number of collocation points is clearly more important than their location.

The effect of the fibre location is shown in Fig. 3(a). Increasing the eccentricity e_n leads to a strong increase in the permeability. A random fibre distribution implies an increase of 75% compared to a perfect fibre distribution, as shown by Fig. 3(b). The fibre content does not influence this behaviour, as also can be observed in both plots of Fig. 2. The normalised

average permeability is defined here as:

$$K_{av} = \frac{\iint_{\Omega_{e_c}} \sigma K(e_c) \mathrm{d}\Omega_{e_c}}{K_{cc} \iint_{\Omega_{e_c}} \mathrm{d}\Omega_{e_c}}, \tag{20}$$

with Ω_{e_c} the domain of possible locations of the center of the inner circle, σ the distribution function (here taken equal to unity) and K_{cc} the permeability for the concentric case.

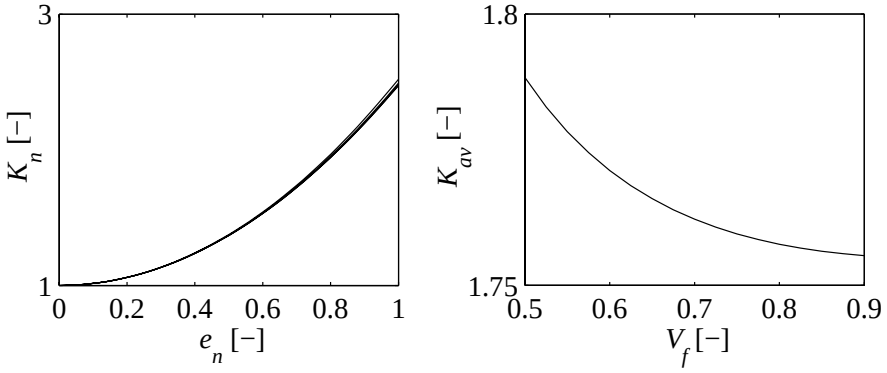

(a) Normalised permeability (b) Normalised average permeability

Fig. 3: Normalised permeabilities as a function of the eccentricity and of the fibre content.

However, a circular domain is no ideal representation of a preform, hence a more suitable domain is analysed: the square domain.

Square Domain

No closed form solution is available for the square domain. A finite element result from the ANSYS/FLOTRAN package is used as a reference. Three dimensional elements with four degrees of freedom per element (three velocities and one pressure) have been used. A value of $8.6{\cdot}10^{-3}\mathrm{m}^2$ has been found for a fibre content of 50% and a = 2m (see Fig. 1). The permeability is now normalised using this value instead of the analytical value.
Again the least square solution has been analysed using various penalty factors P_1 and various numbers of collocation points for the boundary conditions.
In Fig. 4(a) the normalised permeability is depicted as a function of the maximum order of the basic functions for various penalty factors. The number of collocation points is taken high (100 on each boundary). The contribution of the dissipated work (first term in Eqn. 11), smooths the solution, but causes severe underestimation of the permeability for a low order of the basic functions. However, divergence is avoided by the smoothing effect as the order increases, whereas the solution for $P_1 \gg 1$ starts to diverge for higher orders.
Fig. 4(b) shows the influence of the number and location of collocation points on the convergence. Locating a large number of collocation points on the outer boundary (dotted line) gives better results than locating the majority of the points on the inner boundary (solid line), especially for higher order basic functions. When the number of collocation points is taken equal to the number of unknown coefficients of $\{\alpha\}$ and distributed equally over the boundaries (dash-dotted line), convergence is quickly obtained. The accuracy is improved when twice

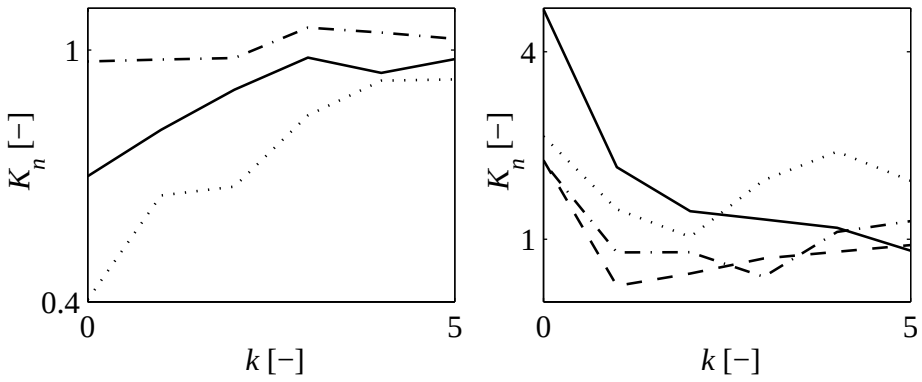

(a) Penalties: - $P_1 = 1$, $\cdots$ $P_1 \ll 1$, -· $P_1 \gg 1$

(b) Number of collocation points on inner and outer boundary: - 3/100, $\cdots$ 100/3, -· minimum, 2×minimum

Fig. 4: The normalised permeability as a function of the order k of the basic functions.

the number of unknown coefficients is used. The results do not seem to improve when more collocation points are used.
Again the permeability has been evaluated as a function of the eccentricity. Based on the above conclusions the penalty P_1 is taken equal to unity, the order k of the basic functions equal to 5. The number of collocation points is taken relatively high to avoid deviations due to a shortage of collocation points.

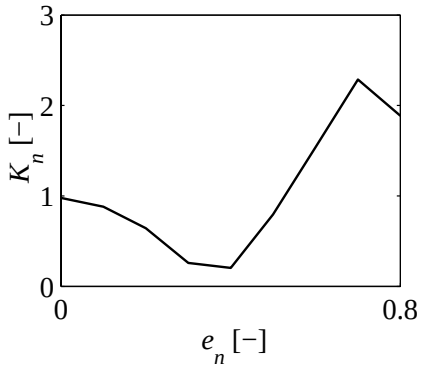

Fig. 5: The normalised permeability as a function of the eccentricity.

Although the solution has to be optimized, the general behaviour, as shown for the circular flow domain, Fig. 3(a), is observed. The decrease in the normalised permeability for eccentricities up to 50%, may be a result of negative velocities, which can occur in the general solution. For higher eccentricities the large ratio between the minimum and maximum distance between the inner and outer boundary causes divergences. Increasing the order of the basic functions and increasing the number of collocation points are likely to improve the results.

CONCLUSIONS

The objective this analysis was to examine the effect of fibre content and fibre distribution on the permeability of RTM preforms. To this end the flow parallel to the fibre in a circular and a square domain was analysed.
The method is fast and converges easily, provided a suitable number of boundary collocation points and suitable penalty factors are chosen. The numerical experiments showed that using a few times the minimum number of collocation points gives acceptable results. With a penalty factor of the order 1 kg·s·m^{-2} the solution converges with increasing order of approximation k, without suppressing the overall flow rate.
The fibre content has hardly any influence on the increase of permeability due to the eccentricity. The effect of the eccentricity on the permeability is shown to be relevant. The average permeability increases up to nearly two times the permeability in the concentric case for the circular shaped flow domain. Similar behaviour is observed for the square domain, although the solution has to be improved yet.
Subsequently a similar approach will be used for the flow transverse to fibres, where again a two-dimensional Stokes flow problem can be analysed. The two components will then be used as the building blocks for permeability analyses of more complicated fibre architectures.

ACKNOWLEDGEMENTS

This work was performed with the support from the National Aerospace Laboratory NLR and the European Commission, by means of the FALCOM project (GRD1-2001-40184). This support is gratefully acknowledged by the authors.

REFERENCES

1. T.S. Lundström, R. Stenberg, R. Bergström, H. Partanen and P.A. Birkeland. “In-plane Permeability Measurements: Stability, Repeatability and Reproducibility”. *Proceedings of ICCM-12*, 1998.

2. S. Bickerton, E.M. Sozer, P. Šimácek and S.G. Advani. “Fabric Structure and Mold Curvature Effects on Preform Permeability and Mold Filling in the RTM Process. Part I. Experiments”. *Composites Part A*, Vol. 31, 2000, pp. 423-438.

3. S. Bickerton, E.M. Sozer, P. Šimácek and S.G. Advani. “Fabric Structure and Mold Curvature Effects on Preform Permeability and Mold Filling in the RTM Process. Part II. Predictions and Comparisons with the Experiments”. *Composites Part A*, Vol. 31, 2000, pp 439-458.

4. T.S. Lundström and B.R. Gebart. “Effect of Perturbation of Fibre Architecture on Permeability Inside Fibre Tows”. *Journal of Composite Materials*, Vol. 29, no.4, 1995, pp. 424-443.

5. N.R.L. Pearce, J. Summerscales and F.J. Guild. “Improving the Resin Transfer Moulding Process for Fabric-Resinforced Composites by Modification of the Fabric Architecture”. *Composites, Part A: Applied Science and Manufacturing*, Vol. 31, 2000, pp. 1433-1441.

6. M.L. Diallo, R. Gauvin and F. Trochu. "Key Factors Affecting the Permeability Measurements in Continuous fiber Reinforcements". *Proceedings of ICCM-11*, 1997.

7. P.B. Nedanov, S.G. Advani, S.W. Walsh and W.O. Ballata. "Determination of the Permeability Tensor of Fibrous Reinforcements for VARTM". *Advances in Aerospace Materials and Structures*, Vol. 58, 1999, pp. 79-88.

8. A. Saouab, J. Bréard, P. Lory, B. Gardarein and G. Bouquet. "Injection Simulations of Thick Composite Parts Manufactored by the RTM Process". *Composites Science and Technology*, Vol. 61, 2001, pp. 445-451.

9. A. Gokce and S. Advani. "Permeability Estimation with the Method of Cells". *Journal of Composite Materials*, Vol. 35, no. 8, 2001, pp. 713-728.

10. T.S. Lundström. "The Permeability of Non-Crimp Stitched Fabrics". *Composites, Part A: Applied Science and Manufacturing*, Vol. 31, 2000, pp. 1345-1353.

11. C. Binétruy, B. Hilaire and J. Pabiot. "The Interactions between Flows Occuring Inside and Outside Fabric Tows during RTM". *Composites Science and Technology*, Vol.57, 1997, pp. 587-596.

12. J. Happel and H. Brenner. "*Low Reynolds Number Hydrodynamics*". Martinus Nijhoff, first (paperback), 1983, ISBN 90-247-2877-0.

13. M.V. Bruschke and S.G. Advani. "Flow of Generalized Newtonian Fluids Across a Periodic Array of Cylinders". *Journal of Rheology*, Vol. 3, no. 37, 1993, pp. 479-498.

14. J.E. Drummond. "Laminar Viscous Flow through Regular Arrays of Paralelle Solid Cylinders". *International Journal of Multiphase Flow*, Vol. 10, no. 5, 1984, pp. 515-540.

15. A.S. Sangani and A. Acrivos. "Slow Flow Past Periodic Arrays of Cylinders with Application to Heat Transfer". *Journal of Multiphase Flow*, Vol. 8, no. 3, 1982, pp. 193-206.

16. F.M. White. "*Fluid Mechanics*". McGraw-Hill International Editions. Mechanical Engineering Series, fourth edition, 1999, ISBN 0-07-116848-6.

17. G.A. Evans, J.M. Blackledge and P.D. Yardley. "*Analytic Methods for Partial Differential Equations*". Springer, 2000, ISBN 3-540-76124-1.